ACTA MECHANICA SINICA (English Series), Vol.17, No.2, May 2001 ISSN 0567-7718
The Chinese Society of Theoretical and Applied Mechanics
Chinese Journal of Mechanics Press, Beijing, China
Allerton Press, INC., New York, U.S.A.

SOME CHARACTERISTICS OF LOW-SPEED STREAKS UNDER SHEARED AIR-WATER INTERFACES*

Wang Shuangfeng (王双峰) Jia Fu (贾 复)
(*Institute of Mechanics, Chinese Academy of Sciences, Beijing* 100080, *China*)

ABSTRACT: The characteristics of low-speed fluid streaks occurring under sheared air-water interfaces were examined by means of hydrogen bubble visualization technique. A critical shear condition under which the streaky structure first appears was determined to be $u_\tau \approx 0.19$ cm/s. The mean spanwise streak spacing increases with distance from the water surface owing to merging and bursting processes, and a linear relationship describing variation of non-dimensional spacing $\overline{\lambda^+}$ versus y^+ was found essentially independent of shear stress on the interface. Values of $\overline{\lambda^+}$, however, are remarkably smaller than their counterparts in the near-wall region of turbulent boundary layers. Though low-speed streaks occur randomly in time and space, the streak spacing exhibits a lognormal probability distribution behavior. A tentative explanation concerning the formation of streaky structure is suggested, and the fact that $\overline{\lambda^+}$ takes rather smaller values than that in wall turbulence is briefly discussed.

KEY WORDS: air-water interface, low-speed streak, turbulent coherent structure, flow visualization

1 INTRODUCTION

Since being discovered as a clue to the existence of ordered structures within a turbulent boundary layer, the longitudinal "streaks" of high- and low-speed fluid have been the subject of persistent and extensive investigations over the past four decades[1,2]. It is now well established that the streaky structure is a fundamental feature of the wall region of all bounded turbulent flows. Kline[3] stressed the ubiquity of streaks and argued that the sublayer streaks exist in any local area where the boundary layer on smooth walls is turbulent and conversely the presence of streaks is a sufficient condition for judging a given flow to be turbulent. Dynamically more interesting is the observation that low-speed streaks often act as apparent locations for the production of turbulent kinetic energy via the subsequent bursting event, which is the dominant agency bringing about turbulent transport processes.

Besides its close relevance to the transport processes of mass, heat and momentum across gas-liquid interfaces, great interest in turbulence behavior near such a boundary is aroused due to the consideration that the particular effect of a gas-liquid interface (compared with a solid wall) can be exploited to improve our understanding of inherent features of turbulent shear flows. In contrast with near-wall turbulence, however, observations and investigations conducted for interface turbulence are much less. Most previous studies in

Received 18 April 2000, revised 30 August 2000
* The project supported by the National Natural Science Foundation of China (19672070)

this research field focused on the interactions between a free-surface (with zero surface shear) and turbulence, as reviewed by Kumar et al.[4]. Rashidi and Banerjee[5] looked at the turbulence structures near a sheared smooth air-water interface in a thin open-channel flow. They reported interesting discoveries : streaky structures and turbulent bursts exist in the vicinity of interface when certain shear rate (about 8~10 s^{-1}) is reached, a quite similar picture to that in wall turbulence. However, the small depth of water flow (the maximum depth was 3.25 cm) used in Rashidi and Banerjee experiments made it difficult to eliminate the interference of bottom wall turbulence. Wang et al.[6] examined the turbulence structures formed independently at sheared air-water interfaces employing a larger water depth in experiments. The visualization study indicated that the wind shear is the chief source for coherent structures near air-water interfaces, and low- and high-speed streaks appear as an outstanding feature of turbulent flows in the vicinity of water surface.

In the present paper, new experimental results concerning such streaky structure are described, and some statistical analyses of the characteristics of low-speed streaks are provided.

2 EXPERIMENTAL METHODS

The experiments were performed in the low turbulence circulating water tunnel in Peking University. Mounted on the Plexiglas working section of the tunnel was a rectangular conduit, through which an air flow was created by an axial-flow fan operating at the downstream end. The wind speed could be varied and controlled by a frequency inverter that regulated the fan. The working section is 3.5 m long, 0.4 m wide by 0.85 m high with water depth of 0.38 m. Observations and measurements were taken at a position 2.0 m downstream from the entrance of air flow. A detailed description of the experimental apparatus can be found in Ref.[6].

The water and air flows were set in opposite directions, and two water flow velocities were adopted in the experiments, $U_\infty = 6.0$ and 13.5 cm/s. The airflow velocities V_∞ were kept under 3.53 m/s so that no significant surface waves would be excited. The wind velocity profiles were accurately measured using a hot-wire anemometer (KANOMAX 1010) with a single-sensor probe (KANOMAX 1026). The sampling frequency and duration were 1 000 Hz and 20 s, respectively. By applying the logarithmic law of velocity distribution, the interface friction velocity v_τ on the air side can be determined, while u_τ on water side was evaluated according to the boundary condition that tangential stresses on two sides of the interface must be equal. Table 1 lists the experimental flow parameters.

Visualization of the streaky structure was done using the hydrogen bubble technique with a platinum wire about 30 μm in diameter, that was located parallel to the air-water interface and normal to the water stream direction. By pulsing the voltage applied on the

Table 1 Summary of the experimental conditions

U_∞ (cm/s)	V_∞ (m/s)	v_τ (cm/s)	u_τ (cm/s)	ν $\times 10^3$(cm^2/s)
6.0	1.74	5.80	0.20	8.63
6.0	2.09	7.57	0.26	9.05
6.0	2.72	10.7	0.37	9.38
6.0	3.12	12.6	0.43	9.17
13.5	2.26	10.8	0.39	8.55
13.5	3.25	14.6	0.50	9.72

wire, hydrogen bubble time-lines can be formed. Through a mechanical mechanism, bubble lines could be introduced parallel to the water surface at any desired depth with an accuracy of 0.01 cm. Flow patterns of the bubble time-lines were viewed directly from the top of the wind-water tunnel and recorded by a CCD camera (25 frames per second) for playback analysis purpose. The video sequences obtained can be further transmitted into a computer to facilitate careful and quantitative examination.

3 EXPERIMENTAL RESULTS

3.1 Appearance of Low- and High-Speed Streaks

Observations indicate that certain magnitude of shear rate imposed on the interface is a prerequisite for the formation of streaky structures under an air-water interface, consistent with the previous report of Wang et al.[6]. In the experiments, the shear rate of air stream was gradually varied, and a critical interface friction velocity was then determined to be $u_\tau \approx 0.19$ cm/s. Figure 1 illustrates typical low- and high-speed streaks. In these pictures

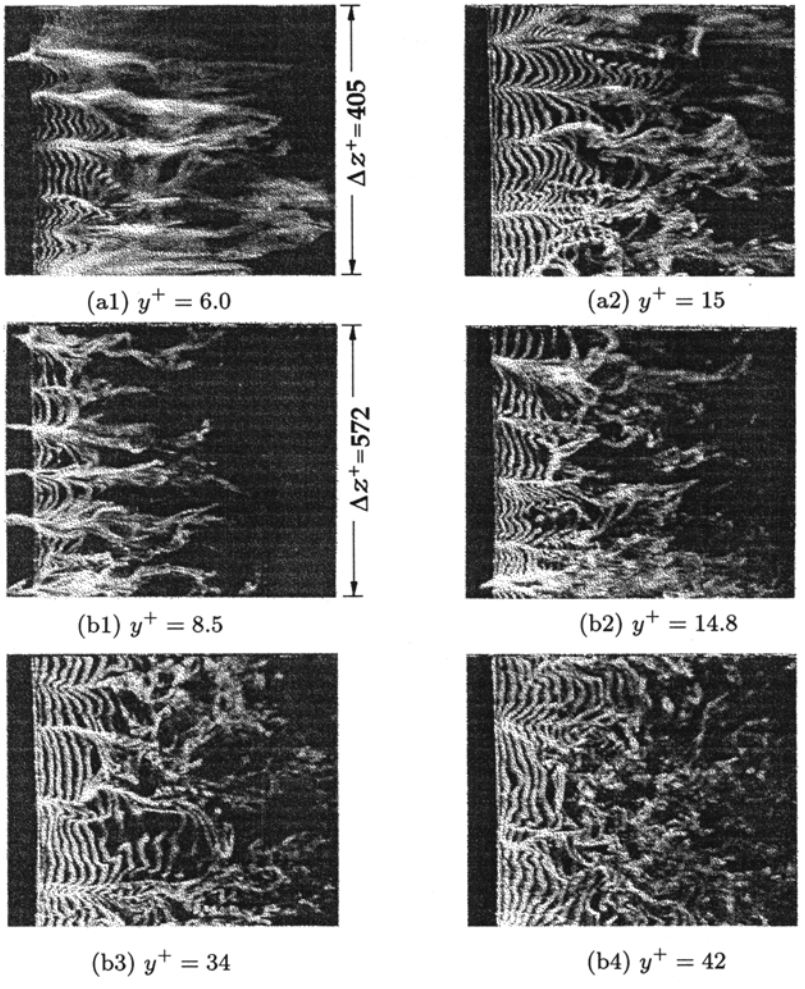

Fig.1 Top views of the streaky structure as visualized with hydrogen bubble time-lines: (a) $u_\tau = 0.26$ cm/s; (b) $u_\tau = 0.37$ cm/s

the flow is from left to right. Both the actual spanwise field of view Δz and the depth of the hydrogen-bubble-wire y are non-dimensionalized using u_τ and the kinematic viscosity ν: $\Delta z^+ = \Delta z u_\tau/\nu$, $y^+ = y u_\tau/\nu$. It can be clearly seen that the basic appearance of streaks is essentially invariant with interface shear stress, and seems similar to those observed in near-wall turbulence. The streaky structure at the interface, however, is somewhat more pronounced than wall streaks with respect to velocity contrast between high-speed and low-speed regions. In the zone closely under the water surface, slow-moving fluid can even reverse temporarily (e.g., in Fig.1(b1)) because of the mobile interface. Beyond $y^+ = 34$ the streaks are not sufficiently well defined to warrant identification.

3.2 Mean Spacing of Low-Speed Streaks

The spanwise spacing between low-speed streaks was determined from the video recording. For each experimental setting, a video sequence of at least 6 000 frames (4 min duration) was recorded, of which a series of 70~100 individual pictures were taken for streak-spacing measurement, with real time interval of $1\frac{1}{5}$ s (30 frames). The data employed for each video sequence ensure that the sample size n_1 of low-speed streak is greater than 300, and the number of streak-spacing value n_2 grater than 230.

The identification of the low-speed regions is generally straightforward. However, during our counting procedure, cases could be encountered where low-speed streaks were weak or less developed. To establish whether these regions would be regarded as a streak, a criterion was set which required that the differential in momentum flux between the adjacent high- and low-speed regions be at least 2 to 1 (or $u_{\text{low}}/u_{\text{high}} < 0.7$), and the streamwise extent of low-speed regions be greater than $\Delta x^+ (= \Delta x u_\tau/\nu) = 100$. The spanwise position of a low-speed streak was determined at $\Delta x^+ = 50$ downstream of the bubble wire. If a streak appeared to terminate, and its upstream end was more than $\Delta x^+ = 50$ downstream of the wire, it was not counted. No restriction was set on a minimum spacing. Only when two streaks had completely merged (i.e., had no well-defined high-speed region between them) would they be counted as one.

Shown in Fig.2 is the non-dimensional average streak spacing $\overline{\lambda^+} = \overline{\lambda} u_\tau/\nu$ versus y^+. The data are for 4 different interface shear conditions. It is evident that $\overline{\lambda^+}$ increases monotonically with increasing y^+ for the experimental conditions examined. Within uncertainties involved in the experiment and image processing procedures a linear law can be fitted as $\overline{\lambda^+} = 1.76y^+ + 61$, which appears independent of the value of interface shear stress. Smith and Metzler[2] demonstrated that in the very-near-wall region of turbulent boundary layers ($y_w^+ \leq 5$) the non-dimensional mean streak spacing $\overline{\lambda_w^+}$ is 100 and invariant with Reynolds number over a rather wide range; whereas for the buffer region of $5 < y_w^+ \leq 30$, $\overline{\lambda_w^+}$ increases with y_w^+ in a similar manner to $\overline{\lambda^+}$ versus y^+. Thus, it can be inferred that, as far as the nondimensionalized distance from boundaries (the wall and the interface) is concerned,

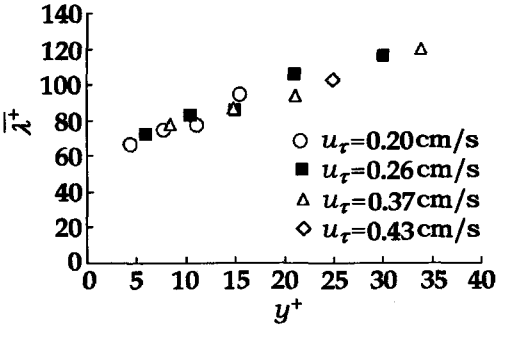

Fig.2 Variation of mean non-dimensional streak spacing with distance from water surface

mean streak spacing $\overline{\lambda^+}$ is much less than $\overline{\lambda_w^+}$, i.e., the spanwise distribution of low-speed streaks is notably denser near an air-water interface than in boundary-layer turbulence. In experiments concerning coherent structure in compliant wall turbulence, Shu and Liu[7] found that the mean streak spacing is smaller than that for rigid wall flow (at $y_w^+ = 10$, $\overline{\lambda_w^+} \approx 82$ and 108, respectively); both these observations suggest a specific effect of boundary conditions on streaks, which will be discussed below.

3.3 Spanwise Distribution of Streaks

Figure 3 presents two typical distribution histograms of spanwise steak spacing. As can be observed, the distributions appear very similar although they are for different interface shear stresses and different hydrogen-bubble-wire locations; both histograms skew toward values lower than the mean, and the most-probable values are less than $\overline{\lambda^+}$. Nakagawa and Nezu[8] and Smith and Metzler[2] showed that the spanwise spacing of low-speed streaks in wall boundary-layer may be described by a lognormal distribution. For the present study this form of probability density function is given by

$$P(\lambda) = \frac{\exp\left[-\frac{1}{2}\left(\frac{1}{\psi_0}\ln\frac{\lambda}{\lambda_0}\right)^2\right]}{\lambda\psi_0(2\pi)^{1/2}} \tag{1}$$

where

$$\lambda_0 = \overline{\lambda}(1+\psi_\lambda^2)^{-1/2} \tag{2}$$

$$\psi_0 = [\ln(1+\psi_\lambda^2)]^{1/2} \tag{3}$$

and ψ_0 is the coefficient of variation of $\ln\lambda$, while λ_0, σ_λ and $\psi_\lambda = \sigma_\lambda/\overline{\lambda}$ denote the median value, standard deviation and coefficient of variation of λ, respectively. From formula (1), lognormal probability-density distributions are evaluated for corresponding statistical $\overline{\lambda}$ and ψ_λ values and superposed over the histograms in Fig.3. The comparison for both distributions shows quite good agreement.

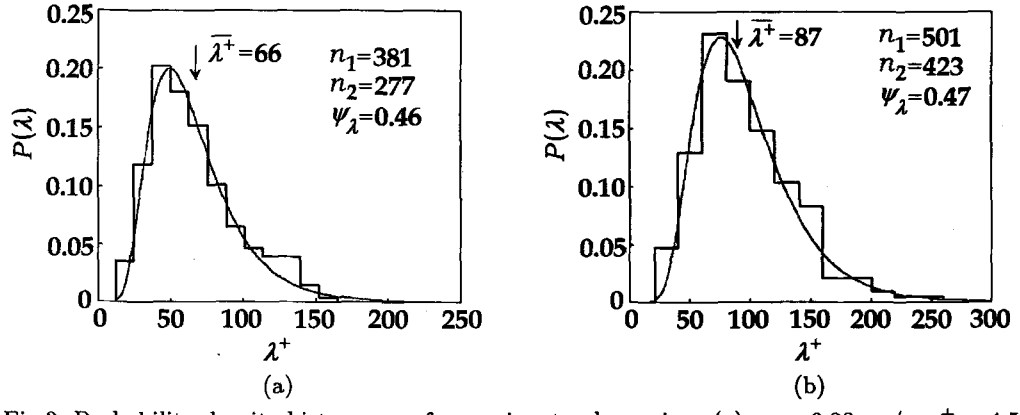

Fig.3 Probability-density histograms of spanwise streak spacing: (a) $u_\tau = 0.20\,\mathrm{cm/s}$, $y^+ = 4.5$; (b) $u_\tau = 0.37\,\mathrm{cm/s}$, $y^+ = 14.8$; ——, lognormal probability density distribution

Figure 4 shows distribution histograms of non-dimensional streak spacing for $u_\tau = 0.26\,\mathrm{cm/s}$ at 4 different depths. Besides the increase in $\overline{\lambda^+}$ with increasing y^+, as mentioned above, the most striking characteristic revealed by Fig.4 is a broadening tendency of the

streak-spacing distribution with increased distance from the water surface. Increase in the standard deviation σ_λ^+ with y^+ is clearly shown in Fig.5, which again displays the broadening streak-spacing distribution.

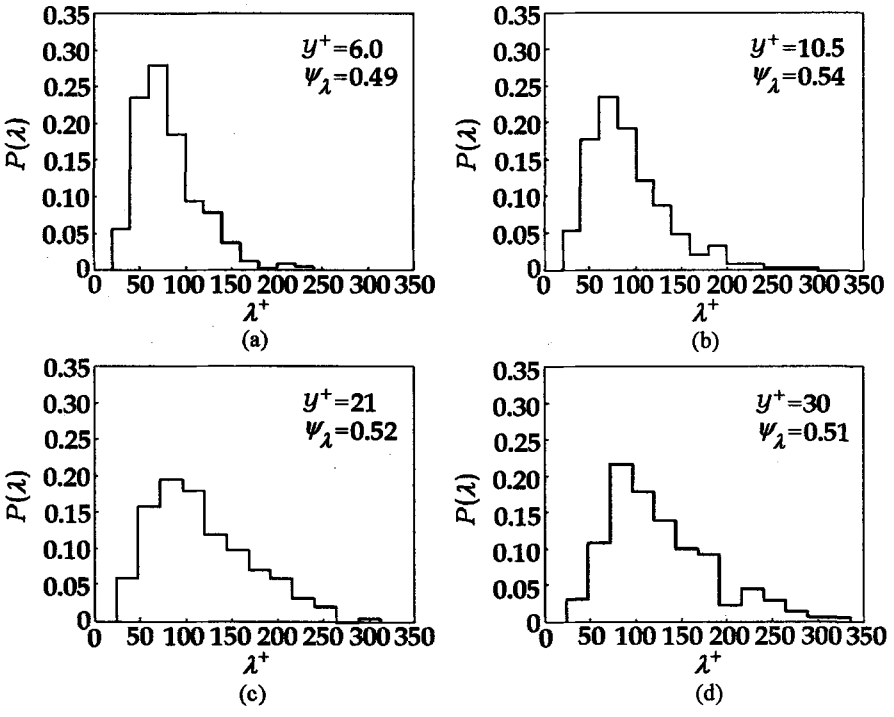

Fig.4 Probability-density histograms of spanwise streak spacing for $u_\tau = 0.26\,\mathrm{cm/s}$

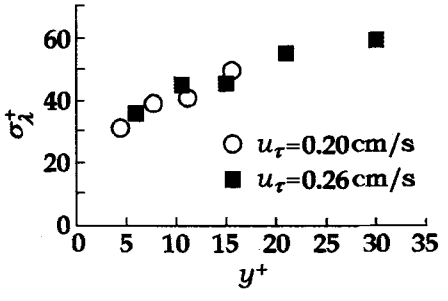

Fig.5 Variation of standard deviation of streak spacing with distance from water surface

To verify further the lognormal behavior of streak-spacing distribution, the data of Fig.3 and Fig.4 are replotted in Fig.6 on a lognormal probability graph of $F(\lambda)$ versus $\lg(\lambda/\overline{\lambda})$, where

$$F(\lambda) = \int_0^\lambda P(\lambda)\mathrm{d}\lambda \tag{4}$$

is the distribution function of streak spacing λ. A true lognormal distribution with $\psi_\lambda = 0.52$ is also shown for comparison. Though the steak-spacing histograms appear to vary from lognormal distribution at the extremes of the graph ($F < 5\%$ and $F > 99\%$), they conform very closely to lognormal behavior over most of the central range. Taking the finite sample size and limited range of spanwise observation window into account, we can be fairly

certain to conclude that the lognormal distribution does satisfactorily represent the shape and characteristics of the streak-spacing histograms, and that it may serve as an appropriate model of low-speed streak spacing in the region $4.5 \leq y^+ \leq 34$.

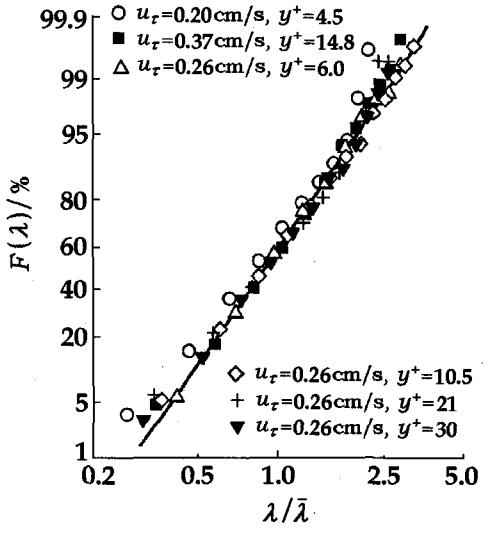

Fig.6 Lognormal probability graph of spanwise streak spacing
—— lognormal probability distribution for $\psi_\lambda = 0.52$

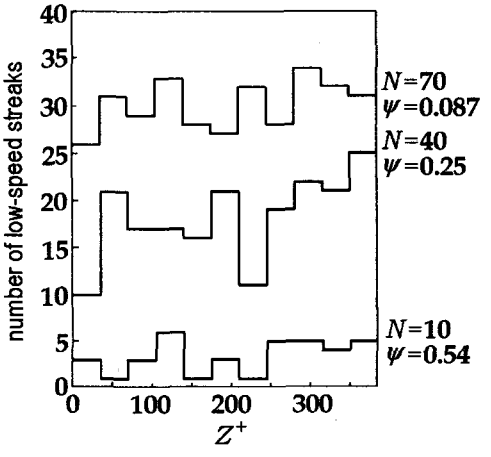

Fig.7 Spanwise distribution of low-speed streaks for $u_\tau = 0.26\,\mathrm{cm/s}$, $y^+ = 6.0$

The streaks occur randomly under a given sheared interface, although this structural feature exists all the while and the low-speed streaks would often tend to maintain their integrity for certain time period. Figure 7 is an example of the spanwise distribution histograms of low-speed streaks. As the number of picture samples N increases from 10 to 70 (with sample time from 12 to 84 s), a more and more balanced histogram, accompanied by a drastic decrease in the coefficient of variation ψ, was obtained. This result indicates that the positions of low-speed streaks do become randomly distributed over a sufficiently long time period, and have not any preferred locations.

3.4 Merging, Splitting and Bursting of Streaks

The low-speed streaks are seldom straight and steady, instead they waver and oscillate all along much like a flag in wind. Consequently the spanwise streak locations can vary greatly. A phenomenon of streak merging was frequently observed in the experiments wherein low-speed streaks approached each other and merged eventually. This merging is most pronounced in the region $10 \leq y^+ \leq 34$. Since the merging process has an effect of reducing the number of independent low-speed regions in the flow, it is an important cause of the increase in streak spacing. Figure 8 is a series of plan-view pictures obtained with the bubble wire at $y^+ = 14.8$, which illustrate a typical merging process. The 4 pictures, which span a time period of $\Delta t^+ (= \Delta t u_\tau^2/\nu) = 32$, show two streaks in the lower part of pictures merging into one low-speed region.

As opposed to merging, a process of streak splitting would also occur, but much less frequently. The splitting appears very transient and usually the divided streaks soon combine

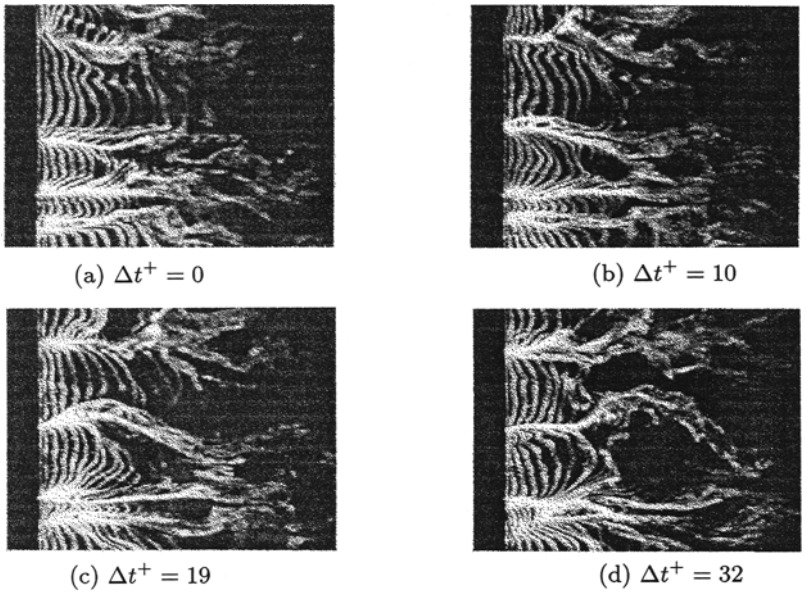

(a) $\Delta t^+ = 0$ (b) $\Delta t^+ = 10$

(c) $\Delta t^+ = 19$ (d) $\Delta t^+ = 32$

Fig.8 Top views of low-speed streaks illustrating a typical merging process $u_\tau = 0.37$ cm/s, $y^+ = 14.8$

again apparently restoring the original streak.

In addition to streak merging, another phenomenon that may bring about larger $\overline{\lambda^+}$ with increasing distance from the interface is the intermittent breakdown or bursting of low-speed streaks. This process was seen clearly in the side views of the flow patterns. Most of the time the low-speed streak extends slowly downstream, with each drifting very slowly downward as well. As a bursting event occurs, the streak breaks down abruptly and becomes intensely contorted and stretched, losing its coherent feature. Furthermore, a portion of it migrates rapidly to the outer edge of the shear layer along an identifiable "trajectory". Since the bursting process flings low-speed fluid from the interface downward into the faster flow, it would inevitably play an important role in energy, momentum and mass transfer between the interface and outer layers.

4 SUMMARY AND DISCUSSION

The results of the present visualization study strongly suggest that, when the shear stress imposed on the water surface becomes greater than a threshold, streaky structures would appear in the boundary flow near an air-water interface. A critical value of the interface friction velocity was determined to be $u_\tau \approx 0.19$ cm/s. Chief features of streaky structures not only remain unchanged for all interface shear stresses investigated, but also show striking similarities with those formed in near-wall turbulence despite the distinctly different boundary conditions at a solid wall and at the interface. It was demonstrated that the occurrence of low-speed streaks is random in space and time, whereas the spanwise streak-spacing can be represented by a lognormal probability distribution. The distribution of λ^+ broadens with increasing y^+.

An increase in the low-speed streak spacing with distance from the interface appears to result from both the merging and bursting of near-interface streaks. For the range of

data available, $\overline{\lambda^+}$ varies linearly with y^+, and the linear relationship seems independent of shear strength at the boundary. This universality implies that u_τ and ν are appropriate scaling parameters for the turbulent flow near sheared air-water interfaces. Concerning the magnitude of mean streak spacing, a rather notable result is that $\overline{\lambda^+}$ is much smaller than the mean streak spacing in wall-bounded turbulence.

$\overline{\lambda_w^+} \approx 100$ is widely accepted for the sublayer zone of a turbulent boundary layer over solid wall, though the physical implication of this specific spacing and its relevance to other coherent motions remain unclear. An opinion now prevailing in turbulence research community (see, e.g., Falco[9] and Smith et al.[10]) believes that low-speed streaks arise as a viscous response of the sublayer to outer region disturbances, which is the pressure distribution induced by a convecting vortex structure in proximity to the wall. As for the vortex configuration in turbulent boundary layers, a variety of models have been put forward by numerous investigators, including inclined hairpin vortices (often referred to as horseshoe vortices)[10~12], vortex rings ("typical eddies")[9] and coherent packets of hairpins[13]. Among these the hairpin vortex, initially proposed by Theodorsen[11] in 1952, has attracted special attention. Theodorsen conjectured, with extraordinary foresight, that hairpin-vortex structure is a common feature of all shear flows, being present not only in wall-bounded flows but also in free shear layers, laminar to turbulent transition and even sheared homogeneous turbulence. Based on their numerical simulations of channel flow, Kim and Moin[14] pointed out, in line with Theodorsen's suggestion, that hairpin vortices is a universal feature of shear flows with or without a wall, and the essential requirement for their formation is the presence of vortex stretching due to strain field. Recent results of direct numerical simulation (DNS) studies on the nature of sheared homogeneous turbulence (see the review of Grass et al.[15]) and on the turbulent shear layer under a free-surface[16] provide powerful new support for Theodorsen's inspired conjectures. In fact, Wang et al.[6] in their experiments observed hairpin vortices appearing in transitional flow under sheared air-water interfaces. The positions of these vortices and the accompanying "turbulent spots" were always seen to coincide with low-speed streak sites. Taken together, all these results justify the application of the hairpin-vortex model to turbulent layers near sheared air-water interfaces.

The hairpins incline at a characteristic angle to the direction of mean flow under air-water interfaces just like in turbulent boundary layers. Once formed, they will undergo continuous stretching in shear flow and hence their strengths are intensely increased. Meanwhile, the trailing legs may move progressively up toward the interface under self-induction action. Such vortical motions would create a local adverse pressure gradient near the interface, which functions as a far-field disturbance to provoke the following evolution of the boundary flow. For wall turbulence Smith et al.[10] argued that a persistent adverse pressure gradient, imposed near the boundary by hairpin vortices, is the key element to produce low-speed streaks in the wall region. It seems that the fundamental behavior of the near-interface layer, responding to this pressure distribution, would bear similarities with the wall flow.

Falco[9] and Smith et al.[10] noted that the details of the vortex-flow interaction depend upon a number of factors; a streak will initiate only when the vortex is sufficiently strong or close to the boundary for a sufficient period of time. Because of the great difference in density and viscosity between the two sides of an air-water interface, the gas phase cannot damp water motions near the interface as effectively as a solid wall does. In particular, the

fluctuations tangential to the interface are left essentially unrestrained (in contrast with a wall boundary where the non-slip condition must be satisfied). Therefore the near-interface flow would be more sensitive to external disturbances than wall flow; when hairpin vortices pass nearby, low-speed streaks have greater likelihood to be produced and sustained under the interface. In other words, hairpin vortices which are relatively weak, far from the water surface or short-lived (can not induce streaks near wall boundary) could give rise to low-speed streaks in near-interface flows. This picture seems to explain the much denser spanwise distribution of low-speed streaks (i.e., $\overline{\lambda^+}$ less than $\overline{\lambda_w^+}$) observed under sheared air-water interfaces.

Acknowledgement The assistance of the State Key Laboratory for Turbulence Research, Peking University, in conducting experiments is gratefully acknowledged.

REFERENCES

1 Kline S J, Reynolds W C, Schraub F A, et al. The structure of turbulent boundary layers. *J Fluid Mech*, 1967, 30: 741~773
2 Smith C R, Metzler S P. The characteristics of low-speed streaks in the near-wall region of a turbulent boundary layer. *J Fluid Mech*, 1983, 129: 27~54
3 Kline S J. A brief history of boundary layer structure research. In: Panton R L ed. Self-Sustaining Mechanisms of Wall Turbulence. Southampton, Boston: Computational Mechanics Publications, 1997. 1~12
4 Kumar S, Gupta R, Banerjee S. An experimental investigation of the characteristics of free-surface turbulence in channel flow. *Phys Fluids*, 1998, 10(2): 437~456
5 Rashidi M, Banerjee S. The effect of boundary conditions and shear rate on streak formation and breakdown in turbulent channel flows. *Phys Fluids*, 1990, 2(10): 1827~1838
6 Wang S F, Jia F, Niu Z N, Wu Z Z. An experimental study on turbulent coherent structures near a sheared air-water interface. *Acta Mechanica Sinica* (English Series), 1999, 15(4): 289~298
7 Shu W, Liu W M. The effect of compliant coatings on coherent structure in turbulent boundary layers. *Acta Mechanica Sinica* (English Series), 1990, 6(2): 97~101
8 Nakagawa H, Nezu I. Structure of space-time correlations of bursting phenomena in an open-channel flow. *J Fluid Mech*, 1981, 104: 1~43
9 Falco R E. A coherent structure model of the turbulent boundary layer and its ability to predict Reynolds number dependence. *Phil Trans R Soc Lond* A, 1991, 336: 103~129
10 Smith C R, Walker J D A, Haidari A H, Sobrun U. On the dynamics of near-wall turbulence. *Phil Trans R Soc Lond* A, 1991, 336: 131~175
11 Theodorsen T. Mechanism of turbulence. In: Proc 2nd Midwestern Conf on Fluid Mech. Ohio State University, Columbus, Ohio, 1952. 1~18
12 Head M R, Brandyopadhyay P. New aspects of turbulent boundary layer structure. *J Fluid Mech*, 1981, 107: 297~338
13 Zhou J, Adrian R J, Balachandar S, Kendall T M. Mechanisms for generating coherent packets of hairpin vortices in channel flow. *J Fluid Mech*, 1999, 387: 353~396
14 Kim J, Moin P. The structure of the vorticity field in turbulent channel flow. Part 2. Study of ensemble-averaged fields. *J Fluid Mech*, 1986, 162: 339~363
15 Grass A J, Stuart R J, Mansour-Tehrani M. Vortical structures and coherent motion in turbulent flow over smooth and rough boundaries. *Phil Trans R Soc Lond* A, 1991, 336: 36~65
16 Tsai W-T. A numerical study of the evolution and structure of a turbulent shear layer under a free surface. *J Fluid Mech*, 1998, 354: 239~276